European Review for Medical and Pharmacological Sciences 2013; 18: 404-412

MRI appearances of stage I_E/II_E extranodal NK/T-cell lymphoma, nasal type, in the upper aerodigestive tract

Y. GU, B. WU, Y. ZHANG, Y. GUO[1], W. PENG

Department of Radiology, Fudan University Shanghai Cancer Center; Department of Oncology, Shanghai Medical College, Fudan University, Shanghai, China
[1]Department of Medical Oncology, Fudan University Shanghai Cancer Center; Department of Oncology, Shanghai Medical College, Fudan University, Shanghai, China

Abstract. – BACKGROUND: The clinical symptoms of NK/T-cell lymphoma at presentation are nonspecific and may mimic those of other benign nasal diseases such as rhinitis and nasal polypus. However, radiologic studies regarding this aggressive clinical course entity are limited.

AIM: To review 123 newly diagnosed MRI appearances in patients with extra-nodal NK/T-cell lymphoma, nasal type, in a large cohort and determine the characteristic imaging findings.

SUBJECTS AND METHODS: We investigated the magnetic resonance imaging (MRI) findings of patients with newly diagnosed stage IE/IIE extranodal NK/T-cell lymphoma, nasal type, in the upper aerodigestive tract.

RESULTS: Most nasal cavity patients (63.4%) showed extra nasal cavity involvements. The polypoid pattern was most frequently seen (55.3%), followed by the infiltrative (27.6%) and combined (17.1%) patterns. The polypoid pattern tended to develop in the nasal cavity group, while the infiltration pattern was more common in the non-nasal cavity group (63.4% vs. 60.0%, $p < 0.001$). Homogeneous iso-intensity was seen in 97.6%, 88.6% and 56.1% of cases on T1-, T2-weighted images and post-contrast images, respectively. Bone destruction and necrosis were observed in 44.7% and 56.3% of patients. Both tumour necrosis and bone destruction were related to tumour size ($p = 0.008$, 0.001). Only 12.2% of patients had cervical lymphadenopathy Multi-region involvement, irregular growth pattern, predisposition to necrosis and bone destruction, and little lymphadenopathy are valuable for diagnosis and can be used to differentiate these tumours from other malignant tumours.

CONCLUSIONS: Our large cohort study of MRI of NK/T cell lymphoma, nasal type, revealed the features of this lymphoma on MRI including some radiologic signs never reported earlier; these findings are invaluable for early diagnosis and may aid future studies aiming to predict the prognosis and response to therapy.

Key Words:
NK/T cell lymphomanasal type, Stage IE/IIE, Magnetic resonance imaging, Upper aerodigestive tract.

Introduction

NK/T cell lymphoma is now definitively categorized in the World Health Organization lymphoma classification system as extra-nodal natural killer (NK)/T-cell lymphoma, nasal-type and a subtype of peripheral T-cell lymphoma[1]. It presents a marked geographic predilection in East Asia, Latin America, and Mexico, while it is rarely observed in the USA or Europe[2]. This tumour mainly occurs in the nasal cavity and possibly develops from a long history of rhinitis. The clinical symptoms at presentation are nonspecific and may mimic those of other benign nasal diseases such as rhinitis and nasal polypus. However, radiologic studies regarding this aggressive clinical course entity are limited. The largest cohort ever reported included only 29 cases including computed tomography (CT) features[3-6]. Moreover, even in primary nasal cavity disease, extra-nasal involvement is common, which is an adverse prognostic factor[7]. Magnetic resonance imaging (MRI) is the first choice for these patients; because of its ability for outstanding soft tissue resolution and multiplanar imaging, it may be easy to differentiate the tumour from normal nasal mucosa or inflammation since either could have the same appearance in CT images[8-9].

The purpose of our study was to review 123 newly diagnosed MRI appearances in patients with extra-nodal NK/T-cell lymphoma, nasal type, in a large cohort and determine the characteristic imaging findings.

Ethics Statement

All the experiments were approved by the Institutional Review Board of Cancer Hospital affiliated to Fudan University. A consent form has

Corresponding Author: Yajia Gu, MD; e-mail: cjr.guyajia@vip.163.com

been written by all participants involved in the study. This study conformed to the Declaration of Helsinki.

Subjects and Methods

Patients

One hundred twenty-three Chinese patients newly diagnosed with early-stage extra-nodal NK/T-cell lymphoma, nasal type, in the upper aerodigestive tract were analyzed. All of the patients underwent MR examination at presentation in our study between July 2005 and December 2009. A total of 123 cases were eligible according to the following inclusion criteria: (1) available head and neck MR examination before therapy, (2) histologically proven, and (3) stage I_E/II_E according to Ann Arbor staging. None of our patients underwent positron emission tomography (PET)/CT examination. Our Institutional Review Board approved this retrospective study with waiver of informed consent.

MRI Interpretation

Images were obtained on a 1.5-T superconducting whole-body MR unit (Signal Infinity Twinspeed Excite, GE, USA) using the multichannel phased-array coil for signal acquisition from the skull base to the thorax inlet. Tumour origin, extent, bone destruction, skin involvement, and cervical lymphadenopathy were evaluated. In size measurement, the response criteria of treatment in Non-Hodgkin's lymphoma were adopted – that is, the maximum radius of the lesion multiplied by the perpendicular one[10]. To analyze the involvement patterns, we classified them into 3 patterns: infiltrative, polypoid, and combined. The infiltrative pattern was defined as when there was diffuse mucosal and submucosal thickening along the walls of the cavity. Localized lesions were defined as presenting a polypoid pattern. Tumours showing both infiltrative and polypoid characteristics were considered to have the combined pattern. Skin enhancement was treated as skin involvement. Bone destruction was characterized as a local disruption of bone with or without mass occupation. We evaluated the cervical lymph node as a positive finding if retropharyngeal lymphadenopathy was present or the lymph node short axial diameter exceeded 10 mm elsewhere in the neck.

The tumours were classified as nasal cavity or non-nasal cavity tumours according to nasal involvement. In the nasal cavity group, we also defined the extra-cavity type as tumour infiltration over one nasal cavity. Tumours with bilateral cavity involvement were classified as the extra-cavity type, but the perforation of the nasal septum without contralateral cavity lesions was not classified as the extra-cavity type. The normal nasal septum showed relative hypointensity on T1- and T2-weighted images, and enhanced images compared with adjacent mucosa. In addition, the perforation status of the nasal septum showed septum discontinuity and replacement by tumour tissue.

The signal intensities of the tumours on T1-weighted imaging with or without contrast were compared with those of the muscles of the infratemporal fossa. The signal intensities of the tumours on T2-weighted imaging were compared with those of the cerebellum on T2-weighted images.

Statistical Analysis

Independent *t*-tests were used to compare the difference between lesion size, and bone destruction and tumour necrosis. The differences in tumour patterns between groups were compared using the chi-squared test. The tumour sizes of the 3 involvement patterns were compared using analysis of variance (ANOVA). The significance value was set at $p \leq 0.05$. All calculations were conducted using statistical software (SPSS version 17.0). Microsoft Excel 2007 spreadsheets were used to record the data.

Results

All patients (95 men and 28 women; age range, 15-79 years; mean, 46 years) underwent MR examination less than 2 weeks before the initiation of treatment.

Size and Location

The lesions ranged from 28-3040 mm^2 with mean and median sizes of 686.3 and 450 mm^2, respectively. The nasal cavity group included 93 patients (75.6%), while the other 30 patients belonged to the non-nasal cavity group. Of the 93 nasal cavity patients, 36.6% (34/93) showed lesions only in one nasal cavity, and 59 (63.4%) showed 152 extra-cavity involvements, ranging from 1-7 other locations (Table I, Figures 1 to 4). Fifty-seven paranasal sinuses involved tumours in 34 patients, including the maxillary (n = 22),

Table I. Extra-cavity involvements in the 59 nasal cavity group patients.

Location	Lesions (%)
Nasopharynx	20 (13.2)
Paranasal sinus	57 (37.5)
Oropharynx	6 (3.9)
Oral cavity	15 (9.9)
Skull base	2 (1.3)
Eye sockets	11 (7.2)
Skin	17 (11.2)
Pterygomaxillary fossa	3 (2.0)
Nasolacrimal canal	5 (3.3)
Contralateral nasal cavity	16 (10.5)
Total	152

ethmoid (n = 31), sphenoid (n = 2), and frontal sinuses (n = 2).

Of the 30 non-nasal cavity patients, 21, 8, and 1 had tumours located at 1, 2, and 3 regions, respectively. A total of 40 regions were involved in this group (Table II; Figures 5, 6). One patient had skin involvement as the only location.

Tumour Patterns and Imaging Features

The polypoid, infiltrative, and combined patterns accounted for 55.3%, 27.6%, and 17.1% of the tumours, respectively (Figures 4, 7, 8). There were significant differences between the 3 patterns between the nasal and non-nasal cavity groups ($\chi^2 = 20.78$, $p < 0.001$). The polypoid pattern was frequently seen in the nasal cavity group, while the non-nasal cavity group had a predilection toward the infiltrative pattern (Table III). The tumour sizes of these 3 patterns were also significantly different (F = 10.481, $p < 0.001$); the combined pattern had the largest mean size (Figure 9).

Before the enhancement, most cases exhibited homogeneous intensity: 97.6% (120/123) and 88.6% (109/123) of cases on T1- and T2-weighted images, respectively. Heterogeneous intensity appeared in only 1 (0.8%) and 12 (9.8%) cases on T1- and T2-weighted images, respectively. Two cases (1.6%) were negative both on T1- and T2-weighted images. No lesions had bright signals in T2-weighted images. In contrast, heterogeneous lesions due to necrotic areas were found in 43.9% of cases (54/123) on post-contrast images (Figure 10). The other 56.1% of patients (69/123) exhibited homogeneous lesions. The 2 cases with no abnormalities seen on T1- or T2-weighted images showed localized laminated homogenous enhancement at the tumour sites (Figure 5). Tumour necrosis was related to tumour size (850.55 mm^2 vs. 549.09 mm^2, $t = 2.716$, $p = 0.008$).

Bone Destruction

Bone destruction was observed in 44.7% of patients (55/123) with 153 bones involved in total (Table IV); the number of pieces ranged from 1-7. Mostly tumour tissue that had replaced bone could be seen. However, 16 lesions located at the nasal concha and 3 lesions located at the septum showed only bone defects without obvious mass, accounting for 12.4% of cases (19/153). This was another characteristic of NK/T cell lymphoma, nasal type. All 16 cases of bilateral nasal cavity involvement had septum bone destruction (Fig-

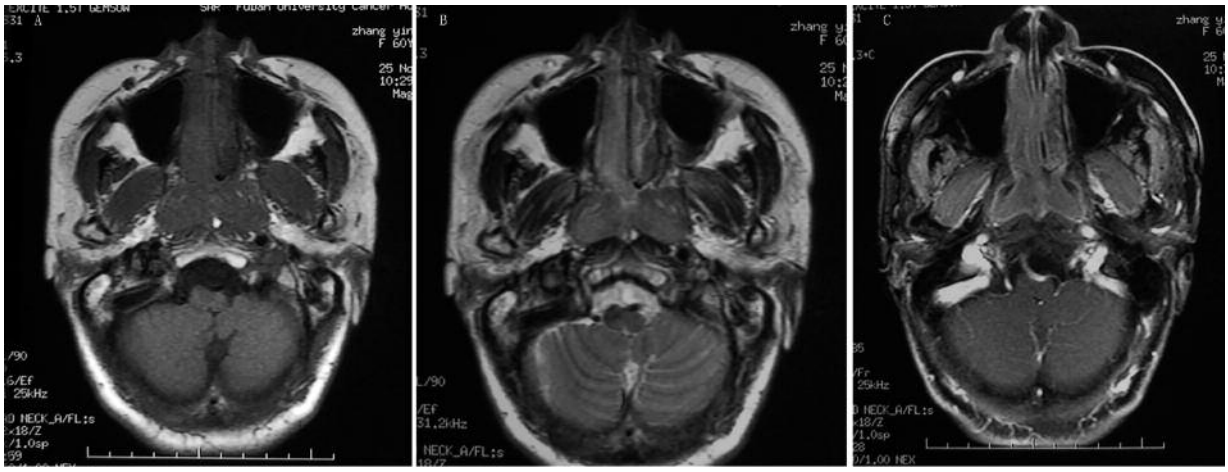

Figure 1. NK/T lymphoma in the right nasal cavity involving the nasopharynx and contralateral nasal cavity. Minor septum bone destruction can be seen on enhanced imaging. The lesion shows homogenous iso-intensity on T1, T2 weighted imaging ***(A, B)*** and post contrast imaging ***(C)***, which is the classic appearance of NK/T lymphoma.

Figure 2. A tumour originating from the left nasal cavity invading both the left maxillary sinus and eye socket.

Figure 4. Combined tumour pattern; the lesion presents both infiltrative and polypoid patterns. Polypoid pattern tumour located at the left nasal cavity (l*ong single arrow*), and infiltrative pattern in the ipsilateral pterygopalatine fossa (*short single arrow*), infratemporal fossa, and nasopharynx (*long twin arrow)*.

ures 7, 8, 10). Bone destruction was also associated with tumour size and was significantly different depending on the existence of bone destruction (935.60 mm^2 vs. 471.08 mm^2, $t = 4.379$, $p < 0.001$).

Figure 3. Primary tumour of the nasal cavity involving the bilateral nasolacrimal canal (*arrow*) with a predilection towards the right side.

Cervical Lymphadenopathy

Fifteen cases (12.2%) exhibited cervical lymphadenopathy. According to the classification of Som et al[11], there were 6 cases of cervical lymphadenopathy restricted to one region including 5 cases in the unilateral level IIA and 1 in the retropharynx region. Among the 5 unilateral level IIA lymphadenopathy cases, the primary lymphoma sites were the ipsilateral nasal cavity in 2 cases, the soft palate in 1 case, both the nasal cavity and the skin involvements in 1 case, and a diffusive lesion that involved the bilateral nasal cavity, nasopharynx, oropharynx, and nasolacrimal canal in 1 case. The oropharynx was the

Table II. Distribution of 40 locations in the 30 non-nasal cavity group patients.

Location	Lesions (%)
Nasopharynx	14 (35.0)
Paranasal sinus	1 (2.5)
Oropharynx	14 (35.0)
Oral cavity	4 (10.0)
Eye sockets	2 (5.0)
Skin	4 (10.0)
Larynx	1 (2.5)
Total	40

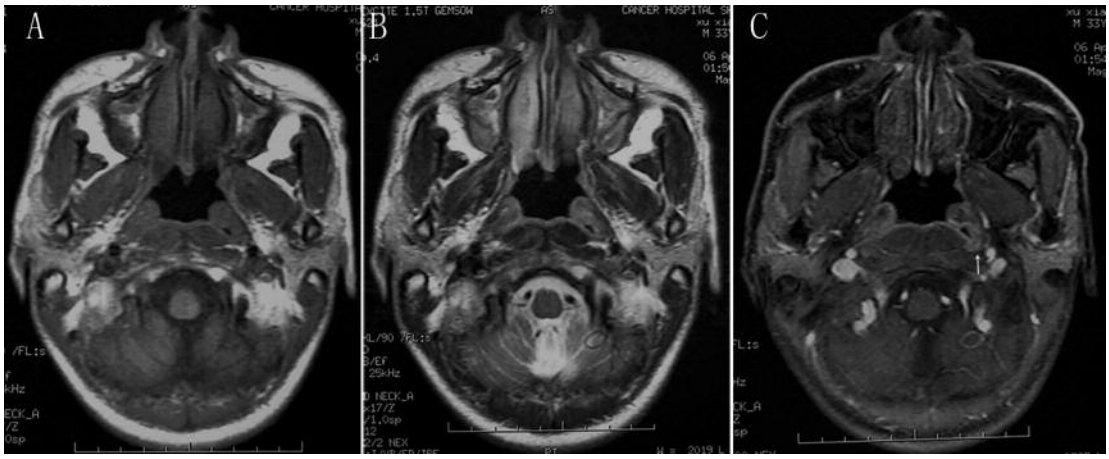

Figure 5. The tumour can be observed as abnormal enhancement ***(C, arrow)*** in the left Rosenmuller's recess with negative appearance in both T1- ***(A)*** and T2-weighted imaging ***(B)***.

primary site of the other patient who had retropharynx adenopathy.

Two or three levels of lymphadenopathy appeared in 7 patients; among them, 3 cases showed bilateral retropharyngeal lymph nodes with the nasopharynx as the primary site in 2 and the bilateral nasal cavity in 1. In the other 4 cases, the lymphadenopathy mainly occurred at level IIA (n = 4), the retropharyngeal area (n = 2), level IB (n = 1), and level III (n = 1).

Diffused lymph node enlargement was observed in 2 cases including 1 covering the entire unilateral neck and supraclavicular region localized primarily in the nasopharyngeal lesion. The other showed multiple levels of lymphadenopathy in both the necks; the primary site in this case extensively involved the nasopharynx, oropharynx, and oral cavity.

The lymph node sizes ranged from 10 × 4 to 32 × 20 mm. Except 2 cases, a few nodes appeared as rim enhancement because of inner necrosis. All others showed homogenous iso-intensity on T1-weighed images and hyperintensity on T2-weighted images compared to the adjacent muscle signal intensity and homogenous enhancement after contrast agent was administrated (Figures 6, 11, 12).

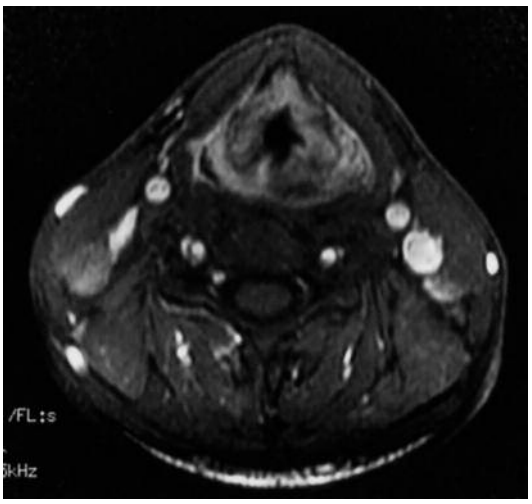

Figure 6. Laryngeal NK/T cell lymphoma presenting with bilateral vocal cord thickening and homogeneous enhancement. Bilateral cervical lymphadenopathy at level III shown in the same image.

Figure 7. Massive bone destruction in the nasal septum accompanied by an obvious mass involving the right forward nasal wing with a polypoid pattern.in the same image.

Figure 8. Defects in both the nasal septum and bilateral nasoturbinal concha without any mass. Infiltrative invasion (*arrow*) can be found in the bilateral nasal wing.

Discussion

Extra-nodal NK/T cell lymphoma, nasal type, is the most common tumour in the nasal cavity in East Asian people. The tumour mainly occurs at the nasal cavity but can be found in other upper aerodigestive tract including the nasopharynx, oropharynx, palate, and larynx. There are a few English-language studies about the imaging appearance of this tumour, particularly MRI[3-6]. However, radiologic studies about this distinct entity are limited. Therefore, we retrospectively reviewed the MRI findings of a large cohort of 123 newly diagnosed cases of extra-nodal NK/T cell lymphoma, nasal type, and determined the characteristic features.

Most previous studies including those with relatively small patient groups report that extra-nodal NK/T cell lymphoma, nasal type, originates from the nasal cavity, spreading to other upper aerodigestive tract regions[3,4,6]. Out of the 123 cases in the present study, most originated from the nasal cavity (75.6%), but 30 cases involved the other upper aerodigestive tract region excluding the nasal cavity. For the nasal cavity group, only 36.6% of cases were limited to one nasal cavity. Most patients exhibited infiltration in the adjacent regions; extra-cavity involvement occurred in 1-7 regions. The paranasal sinus was the most frequent extra-cavity involvement site (37.5%) – more common than the nasopharynx and oropharynx (total, 17.1%). The ethmoid sinus was the most frequently involved; combined with the maxillary sinus, these 2 sites accounted for 93.0% (53/57) of all paranasal sinus involvement. These results are consistent with those of Ou et al[3] but contradict those of King et al[4] and Kim et al[5] who found that the nasopharynx and oropharynx are involved more frequently. Skin involvement was rare. Little involvement was found in the eye sockets, nasolacrimal canal, dental alveoli, skull base, hard palate, sphenoid sinus, and frontal sinus. Involvement in the nasolacrimal canal, sphenoid sinus, and frontal sinus is not reported in the literatures.

For the non-nasal cavity group, lesions were mostly restricted to one region (70%). The nasopharynx and oropharynx were the mostly frequent locations with 35% each, followed by the oral cavity, skin, eye sockets, paranasal sinus, and larynx in decreasing order. Kim et al[5] also report 3 cases of upper aerodigestive tract NK/T cell lymphoma without nasal cavity involvement. Skin involvement as a unity location was not common and usually existed as an accompany finding.

The contours of most NK/T cell lymphomas were irregular. They can be mildly swollen if they involve the nasal concha and exhibit abnormal signal intensity changes compared to those of normal conditions. Tumour in other locations could also be identified by asymmetric morphology, signal intensity changes, and necrosis inside

Table III. Pattern in the nasal and non-nasal cavity groups.

	Nasal cavity group n (%)	Non-nasal cavity group n (%)	Totaln (%)
Polypoid	59 (63.4)	9 (30.0)	68 (55.3)
Infiltrative	16 (17.2)	18 (60.0)	34 (27.6)
Combined	18 (19.4)	3 (10.0)	21 (17.1)
Total	30	93	123

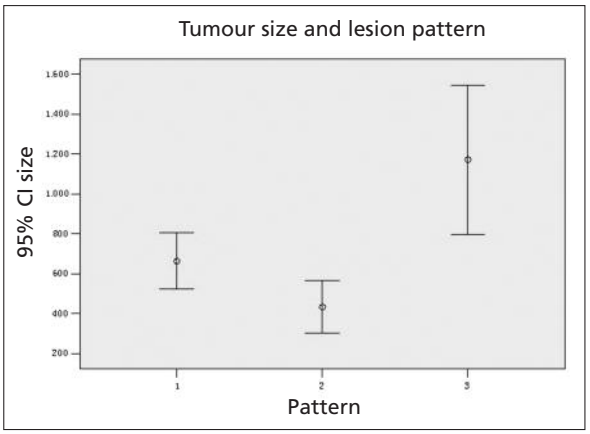

Figure 9. The tumour sizes of different patterns: 1, polypoid; 2, infiltrative; 3, combined. The combined pattern tumours were the largest.

Table IV. Distribution of the 153 sites of bone destruction in 55 cases.

Location	Lesions (%)
Nasal septum	24 (15.7)
Inferior nasal concha	27 (17.6)
Middle nasal concha	27 (17.6)
Alveolus dentis	3 (2.0)
Maxillary sinus	21 (13.7)
Ethmoid sinus	30 (19.6)
Eye sockets	8 (5.2)
Sphenoid sinus	2 (1.3)
Frontal sinus	2 (1.3)
Nasolacrimal canal	4 (2.6)
Hard palate	2 (1.3)
Skull base	3 (2.0)
Total	153

the lesion. Some tiny lamellar lesions could only be seen in post-contrast images. It is essential to make exact evaluations with detailed observations of every planar image and sequence. The polypoid pattern was the most common in our study, particularly in the nasal cavity group; this contrasts with the results of Kim et al[5] who report that 69% of 26 nasal cavity involvement cases had an infiltrative pattern. We had a relatively higher incidence of the infiltrative type in non-nasal cavity group (60.0%), which manifested as diffuse mucosal and submucosal thickening along the walls of the cavity. Overall, the combined pattern had the largest tumour size among the 3 growth patterns; this indicates that in some patients, this may represent the progress of the lesion. Meanwhile, the infiltrative region in the combined pattern is the result of necrotic defects.

Figure 10. NK/T cell lymphoma in the bilateral nasal cavity. The normal bone is replaced by tumour tissue (*arrow*) with mild destruction in the nasal septum. The heterogeneous signal intensity of the left wing indicates tumour involvement.

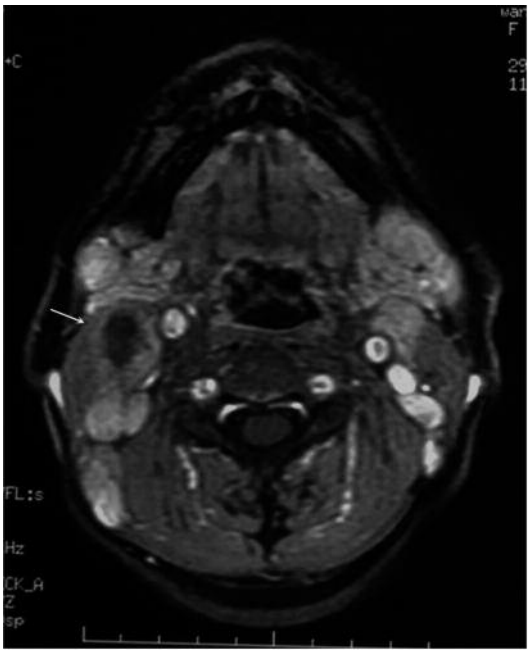

Figure 11. Multiple bilateral cervical lymphadenopathy with a homogenous signal intensity was found in most lymph nodes. Rim enhancement (*arrow*) in one of the right cervical lymphadenopathies due to inner necrosis.

Figure 12. Bilateral retropharyngeal lymphadenopathy (arrow); the primary lymphoma site is located in the oropharynx.

The present findings are corroborated by those King et al[4] in that most tumours showed homogenous signal intensity in T1- and T2-weighted images; in addition, over half of the tumours were homogenously enhanced after the contrast agent was administrated. However, other authors including Ou et al[3] and Ooi et al[6] report heterogeneous enhancement in most cases, which differs from our results. Necrosis is common in NK/T cell lymphoma, especially when the tumour is large. Such necrosis was liable to be seen clearly with heterogeneous signal intensity on post-contrast images (43.9%) but scarcely seen on pre-enhanced T1-weighted images. Only a few cases with necrosis (9.8%) appeared on T2-weighted images with no marked hyperintensity as usual. This can be explained according to the special conditions of necrosis – in other words, it could be a unique sign of NK/T cell lymphoma. The other typical change in necrosis is the destruction of involved anatomic structures without mass, which is hardly seen in other malignant tumours affecting the nasal cavity.

Bone destruction is reported in 17.0-77.8% of cases in the literature[2,3,5,6]. The 44.7% of cases exhibiting bone destruction in our study is in agreement with that reported by Cheung et al[2]; bone destruction occurred in 1-7 bones. The ethmoid sinus was the most frequently involved, followed by the middle and inferior nasal concha, nasal septum, and maxillary sinus; this contrasts with the results of Ooi et al[6] and Ou et al[3] who report the maxillary sinus as the most common site. The main appearances of bone destruction on MRI are the replacement of normal bone signal intensity with that of tumour tissue. However, 12.4% of lesions showed bone defects without massive tumours; these were mainly found at the nasal concha and nasal septum. Mild laminated enhancement can be found in such regions, demonstrated only on coronal position in some cases, making it unique to other tumours involving the nasal cavity.

Kim et al[7] demonstrated that bone destruction and skin involvement are the 2 most important prognostic factors for predicting low probability of complete remission (CR), reduced overall survival (OS), and disease-free survival (DFS) in nasal stage I/II NK/T cell lymphoma. The results of the present study confirm that MRI is a valuable tool for detecting these changes. Cervical lymphadenopathy was uncommon (12.2%) in the upper aerodigestive tract in nasal-type NK/T cell lymphoma in this study, which is very similar to that reported by Ou et al[3]. Cervical lymphadenopathy may be an adverse factor affecting prognosis such as 'B' symptom, stage, and lactate dehydrogenase (LDH) level[12]. In our study, the lymphadenopathies were mostly homogeneous and occurred in level IIA and the retropharynx region.

MRI of the upper aerodigestive tract in nasal-type NK/T cell lymphoma may have some characteristic appearances, but differentiated diagnosis is especially imperative for the following head and neck tumours. (1) Squamous cell carcinoma is the most common malignant tumour in the head and neck region, and is likely to be visualized as a large mass with massive bone destruction. (2) Adenoid cystic carcinoma is a rare tumour originating from the small salivary glands; invasive and irregular submucosal invasion is the main growth pattern. The classical MRI appearances include hyperintensity lesions with septa on T2-weighted images and heterogeneous enhancement with cystic changes on post-contrast images. Perineural spread is another unique sign[13]. (3) Wegener granulomatosis, especially advanced Wegener granulomatosis may lead to massive destructive lesions of the hard palate, nasal septum, and paranasal sinuses. The disease may affect the eyes, skin, joints, muscles, and

cardiac system as well as the lungs and kidneys. It commonly involves the nervous system, usually taking the form of peripheral or cranial neuropathy, which is rarely seen in NK/T cell lymphoma[14]. (4) Olfactory neuroblastoma is a rare tumour that may originate from the ethmoid plate near the superior nasal meatus. Localized bone destruction can be found frequently, and CT can show calcification within the tumour. Clinical symptoms include hyposmia or anosmia[14]. (5) The most common site of mycotic paranasal rhinosinusitis is the maxillary sinus, but all paranasal sinuses can be involved. Chronic rhinosinusitis takes a long time, favouring bone remoulding rather than destruction. The signal intensity is complex for the metal deposits inner the lesion[15,16].

Conclusions

Our large cohort study of MRI of NK/T cell lymphoma, nasal type, revealed the features of this lymphoma on MRI including some radiologic signs never reported earlier; these findings are invaluable for early diagnosis and may aid future studies aiming to predict the prognosis and response to therapy.

Conflict of Interest

The Authors declare that there are no conflicts of interest.

References

1) Chan JKCJE, Ralfkiaer E. Extranodal NK/T-cell lymphoma, nasal type. In: Jaffe ES, Harris NL, Stein H, Vardiman JW, editors. World Health Organization classification of tumours: pathology and genetics of tumors of hematopoietic and lymphoid tissues. Lyon, France: IARC Press 2001; 20, pp. 4-207.
2) Cheung MM, Chan JK, Lau WH, Foo W, Chan PT, Ng CS, Ngan RK. Primary non-Hodgkin's lymphoma of the nose and nasopharynx: clinical features, tumor immunophenotype, and treatment outcome in 113 patients. J Clin Oncol 1998; 16: 70-77.
3) Ou CH, Chen CC, Ling JC, Chai JW, Wu CH, Chen WH, Hung HC, Lee T, Ho TL. Nasal NK/T-cell lymphoma: computed tomography and magnetic resonance imaging findings. J Chin Med Assoc 2007; 70: 207-212.
4) King AD, Lei KI, Ahuja AT, Lam WW, Metreweli C. MR imaging of nasal T-cell/natural killer cell lymphoma. AJR 2000; 174: 209-211.
5) Kim J, Kim EY, Lee SK, Kim DI, Kim CH, Kim SH, Choi EC. Extranodal nasal-type NK/T-cell lymphoma: computed tomography fingdings of head and neck involvement. Acta Radiol 2010; 51: 164-169.
6) Ooi GC, Chim CS, Liang R, Tsang KW, Kwong YL. Nasal T-cell/natural killer cell lymphoma: CT and MR imaging features of a new clinicopathologic entity. AJR 2000; 174: 1141-1145.
7) Kim TM, Park YH, Lee SY, Kim JH, Kim DW, Im SA, Kim TY, Kim CW, Heo DS, Bang YJ, Chang KH, Kim NK. Local tumor invasiveness is more predictive of survival than International Prognostic Index in stage IE/IIE extranodal NK/T-cell lymphoma, nasal type. Blood 2005; 106: 3785-3790.
8) Ng SH, Chang TC, Ko SF, Yen PS, Wan YL, Tang LM, Tsai MH. Nasopharyngeal carcinoma: MRI and CT assessment. Neuroradiology 1997; 39: 741-746.
9) McCabe KJ, Rubinstein D. Advances in head and neck imaging. Otolaryngol Clin N Am 2005; 38: 307-319.
10) Cheson BD, Horning SJ, Coiffier B, Shipp MA, Fisher RI, Connors JM, Lister TA, Vose J, Grillo-López A, Hagenbeek A, Cabanillas F, Klippensten D, Hiddemann W, Castellino R, Harris NL, Armitage JO, Carter W, Hoppe R, Canellos GP. Report of an international workshop to standardize response criteria for non-hodgkin's lymphomas. NCI Sponsored International Working Group. J Clin Oncol 1999; 17: 1244.
11) Som PM, Curtin HD, Mancuso AA. Imaging-based nodal classification for evaluation of neck metastatic adenopathy. AJR 2000; 174: 837-844.
12) Lee J, Suh C, Park YH, Ko YH, Bang SM, Lee JH, Lee DH, Huh J, Oh SY, Kwon HC, Kim HJ, Lee SI, Kim JH, Park J, Oh SJ, Kim K, Jung C, Park K, Kim WS. Extranodal natural killer T-cell lymphoma, nasal-type: a prognostic model from a retrospective multicenter study. J Clin Oncol 2006; 24: 612-618.
13) Gu YJ, Wu B, Yang WT. The MR imaging appearances of head and neck adenoid cystic carcinoma correlation with pathological results. Chinese Med Comput Imag 2008; 14: 100-105.
14) Valencia MP, Castillo M. Congenital and acquired lesions of the nasal septum: a practical guide for differential diagnosis. Radiographics 2008; 28: 205-224.
15) Eggesbø HB. Radiological imaging of inflammatory lesions in the nasal cavity and paranasal sinuses. Eur Radiol 2006; 16: 872-888.
16) Maroldi R, Ravanelli M, Borghesi A, Farina D. Paranasal sinus imaging. Eur J Radiol 2008; 66: 372-386.